NUMERICAL ANALYSIS OF ACCURACY FOR EVOLUTIONARY ANISOTROPIC PLASTICITY MODELS

Vedrana Cvitanić[*] - Maja Kovačić - Antonio Vladislavić

Department of Mechanical Engineering and Naval Architecture, Faculty of Electrical Engineering, Mechanical Engineering and Naval Architecture, University of Split, Ruđera Boškovića 32, 21000 Split, Croatia

ARTICLE INFO

***Article history*:**
Received: 7.12.2015.
Received in revised form: 15.2.2016.
Accepted: 15.2.2016.

Keywords:
Sheet metals
Constitutive modeling
Anisotropy evolution
Implicit return mapping
Iso-error maps

Abstract:

In the present paper, elasto-plastic constitutive formulations based on the orthotropic four parametric quadratic Hill (1948) or non-quadratic Karafillis-Boyce (1993) stress function and distortional evolution of the yield function/plastic potential are presented. The anisotropy parameters of the analyzed yield functions/plastic potentials are introduced as functions of the equivalent plastic strain. The formulations are developed and analyzed considering experimental data for the selected steel sheet sample with reported significant variation of the instantaneous Lankford parameter with straining. Predictions of the directional dependences and variations with straining of the yield stress ratios and Lankford parameters obtained by the presented descriptions are considered. The algorithmic formulations of the analyzed constitutive descriptions are derived by application of the implicit return mapping algorithm. In order to estimate accuracy of the developed algorithms, iso-error maps are calculated and analyzed.

1 Introduction

Sheet metals exhibit initial plastic anisotropy induced mainly due to the production rolling steps as well as deformation plastic anisotropy induced during the forming process. In other words, plastic anisotropy in sheet metals changes with the continuation of the plastic deformation process. The common approach in phenomenological plasticity models intended for sheet metals is based on the orthotropic yield function/plastic potential with fixed anisotropy parameters. These parameters are calculated using the initial yield stress ratios and/or constant Lankford parameters. Lankford parameter (*r*-value, plastic strain ratio) is used as the measure of plastic flow and is defined as the ratio of the sheet specimen transverse and thickness true plastic strain increments in uniaxial tensile testing. According to the standards, this parameter is calculated by the linear regression of the transverse versus longitudinal plastic strain plot between certain limits of the measured strains. Therefore, it is considered as constant value regardless of the accumulation of the plastic strain. Assuming fixed yield stress ratios and Lankford parameters, i.e., by using fixed anisotropy parameters, any possible distortion of the yield function/plastic potential is disabled. That means that any possible evolution of

[*] Corresponding author. Tel.: +385 21 305 970
E-mail address: vcvit@fesb.hr.

the plastic anisotropy with continuation of the plastic deformation process is neglected.

Some recent experimental studies report alternation of the yield stress ratios and/or instantaneous *r*-values with evolution of sheet crystallographic texture during deformation process [1], [2], [3]. Furthermore, numerous studies related to the application of the orthotropic plasticity formulations with constant anisotropy parameters in predicting complex forming processes indicate that possible model improvements could be achieved by incorporating the evolution of yield stress ratios and *r*-values into the model. This is particularly evident in the simulations of the cylindrical cup drawing problem, see for instance [4], [5]. Recently, constitutive formulations based on the multiple strain hardening curves and fixed *r*-values were developed and improved predictions of the material behavior are reported [6], [7], [8]. Therefore, it can be concluded that reliable sheet metal constitutive model should be capable of predicting the evolution of the plastic anisotropy and that the anisotropy parameters of the yield function/plastic potential should be altered by certain measure of the plastic deformation process.

In the present paper, constitutive formulations based on associated or non-associated flow rule and orthotropic four parametric quadratic Hill (1948) stress function [9] or non-quadratic Karafillis-Boyce (1993) stress function [10] that assume distortion of the yield function/plastic potential are considered. For the numerical implementation, the algorithmic formulations of the analyzed constitutive descriptions are derived by the application of the implicit return mapping algorithm. The constitutive descriptions are developed and analyzed by considering experimental data for DC06 steel sheet presented by Safaei et al. [3]. In their work, Safaei et al. reported significant decrease of *r*-value and certain variation of the yield stress ratios with straining in uniaxial tensile testings for DC06 sheet. They considered the non-associated model based on eight parametric Yld2000-2d stress function [11] with anisotropy parameters adjusted to the yield stresses and *r*-values determined for seven uniaxial specimen orientations and balanced biaxial stress state. Furthermore, they introduced the interpolation technique to express the evolution of anisotropy parameters with respect to the equivalent plastic strain and analyzed capability of the developed formulation to predict yield function/plastic potential distortion with ongoing deformation process. The non-associated formulations based on four parametric stress functions that are analyzed in this paper require fewer numbers of the experimental data in the calibration procedure. The paper is organized as follows. The orthotropic Hill (1948) and Karafillis-Boyce (1993) stress functions are presented in Section 2. In Section 3, experimental data for DC06 sheet steel are presented and evolutionary anisotropic constitutive models based on the analyzed stress functions are considered. The capabilities of the analyzed formulations to predict directional dependence and evolution of the uniaxial plastic properties for the considered sheet material are analyzed. In Section 4, algorithmic formulations of the proposed constitutive descriptions based on associated flow rule are derived by application of the implicit return mapping algorithm. In order to estimate accuracy of the developed algorithms, iso-error maps are calculated.

2 Hill stress function and Karafillis-Boyce stress function

The analyzed evolutionary constitutive formulations utilize yield function/plastic potential with functional form of the orthotropic Hill (1948) function [9] or Karafillis-Boyce (1993) function [10]. In sheet metal forming, it is a common practice to assume that the sheet is approximately subjected to plane stress conditions and that material exhibits orthotropic symmetry in plastic properties. Therefore, the analyzed yield functions/plastic potentials are stated as functions of in-plane stress components, σ_{xx}, σ_{yy} and σ_{xy}, where *x*-axis denotes the original sheet rolling direction and *y*-axis denotes the direction in sheet plane transverse to the rolling direction. The *z*-axis denotes the sheet normal direction.

The orthotropic Hill (1948) stress function is a quadratic function derived as an extension of the isotropic von Mises yield function. For plane stress conditions, Hill (1948) stress function can be written in the following form

$$f_y = \sqrt{\lambda_1 \sigma_{xx}^2 + \lambda_2 \sigma_{yy}^2 - 2\nu \sigma_{xx} \sigma_{yy} + 2\rho \sigma_{xy}^2} = \sigma_y \quad (1)$$

In the above expression, λ_1, λ_2, ν and ρ are anisotropic material parameters that can be adjusted to experimental data and σ_y is the yield stress for the referent direction.

The orthotropic Karafillis-Boyce (1993) stress function is a linear combination of two convex non-quadratic functions

$$f_y = (\frac{(1-c)}{2}\left((\tilde{s}_1-\tilde{s}_2)^m+(\tilde{s}_2-\tilde{s}_3)^m+(\tilde{s}_3-\tilde{s}_1)^m\right)+ \\ +\frac{c}{2}\frac{3^m}{\left(2^{m-1}+1\right)}\left((\tilde{s}_1)^m+(\tilde{s}_2)^m+(\tilde{s}_3)^m\right))^{1/m}=\sigma_y \tag{2}$$

where exponent m is an even number and c is a weightening parameter. In Eq. (2) $\tilde{s}_1, \tilde{s}_2, \tilde{s}_3$ are the principal values of the so called isotropic plasticity equivalent stress tensor. For plane stress conditions these values can be calculated as

$$\tilde{s}_{1,2}=\frac{\tilde{s}_{xx}+\tilde{s}_{yy}}{2}\pm\sqrt{\left(\frac{\tilde{s}_{xx}-\tilde{s}_{yy}}{2}\right)^2+\tilde{s}_{xy}^2}, \quad \tilde{s}_3=\tilde{s}_{zz} \tag{3}$$

where

$$\begin{Bmatrix}\tilde{s}_{xx}\\ \tilde{s}_{yy}\\ \tilde{s}_{zz}\\ \tilde{s}_{xy}\end{Bmatrix}=C\begin{bmatrix}1 & \beta_1 & \beta_2 & 0\\ \beta_1 & \alpha_1 & \beta_3 & 0\\ \beta_2 & \beta_3 & \alpha_2 & 0\\ 0 & 0 & 0 & \gamma_3\end{bmatrix}\begin{Bmatrix}\sigma_{xx}\\ \sigma_{yy}\\ \sigma_{zz}=0\\ \sigma_{xy}\end{Bmatrix} \tag{4}$$

and

$$\beta_1=\frac{\alpha_2-\alpha_1-1}{2}, \beta_2=\frac{\alpha_1-\alpha_2-1}{2}, \beta_3=\frac{1-\alpha_1-\alpha_2}{2} \tag{5}$$

The constants $C, \alpha_1, \alpha_2, \gamma_3$ are anisotropic parameters. For isotropic material, these parameters have the values $C=2/3$, $\alpha_1=\alpha_2=1$, $\gamma_3=3/2$, and stress components defined by Eq. (4) reduce to the components of the stress deviator tensor.

Under the associated flow rule, the analyzed functions act as yield function as well as plastic potential, therefore, they can be adjusted to the yield stresses or experimental data indicating plastic flow. In the non-associated formulation, parameters of the Hill (1948) or Karafillis-Boyce (1993) yield function are defined in terms of three directional yield stresses obtained in the uniaxial tension of the specimens oriented at 0°, 45° and 90° to the rolling direction and equibiaxial yield stress. The associated yield stresses are denoted as σ_0, σ_{45}, σ_{90} and σ_b. The parameters of the Hill (1948) or Karafillis-Boyce (1993) plastic potential are defined in terms of experimental data indicating plastic flow such as Lankford parameter that reads

$$r=\frac{d\varepsilon_{22}^p}{d\varepsilon_{33}^p} \tag{6}$$

where $d\varepsilon_{22}^p$ and $d\varepsilon_{33}^p$ are width and thickness plastic strain rate, respectively, obtained in uniaxial sheet specimen tension. In calculating parameters of the plastic potential, three plastic strain ratios obtained in the uniaxial tensions along 0°, 45° and 90° to the rolling direction and the yield stress for the referent direction σ_0 are used. The associated plastic strain ratios are denoted as r_0, r_{45} and r_{90}. For Hill (1948) stress function calculation procedure results in the explicit expressions for anisotropy parameters. The parameters of the Hill (1948) function adjusted to the yield stresses read

$$\lambda_1=1, \quad \lambda_2=(\sigma_0/\sigma_{90})^2, \\ \nu=0.5(1+(\sigma_0/\sigma_{90})^2+(\sigma_0/\sigma_b)^2), \\ \rho=2(\sigma_0/\sigma_{45})^2-0.5(\sigma_0/\sigma_b)^2 \tag{7}$$

If the Hill (1948) function is adjusted to the plastic strain ratios following expresions are obtained

$$\lambda_1=1, \ \lambda_2=\frac{1+1/r_{90}}{1+1/r_0}, \ \nu=\frac{1}{1+1/r_0}, \\ \rho=\frac{(1+2r_{45})(1/r_0+1/r_{90})}{2(1+1/r_0)} \tag{8}$$

Calculation of the anisotropy parameters of the Karafillis-Boyce (1993) stress function leads to the system of non-linear equations that can be solved using a numerical iterative procedure.

3 Evolutionary anisotropic constitutive models

3.1 Experimental data for DC06 steel sheet

The analyzed evolutionary anisotropic constitutive models are developed and analyzed considering experimentally determined directional dependences

Table 1. Parameters of the combined Swift-Voce hardening law for DC06 steel sheet [3]

$\theta(^\circ)$	k	$\bar{\varepsilon}_0^p$	n	c'	Q	b	R
0	539.542	0.012	0.326	0.848	557.223	34.822	29.247
15	669.128	0.092	0.535	0.649	408.320	25.302	14.290
30	488.056	0.000	0.390	0.468	288.963	13.258	209.536
45	581.667	0.024	0.946	0.644	457.245	22.122	325.168
60	617.050	0.257	1.000	0.593	410.000	21.844	82.687
75	586.481	0.042	1.000	0.624	454.761	21.635	298.764
90	637.222	0.062	0.937	0.568	381.940	21.593	239.494

of the uniaxial material properties and their evolution with ongoing deformation process for DC06 steel sheet reported by Safaei et al. [3].

The utilized data are related to uniaxial straining tests of the seven sheet specimens with orientations 0°, 15°, 30°, 45°, 60°, 75° and 90° to the rolling direction. For each specimen following data are reported: 1) parameters of the combined Swift-Voce hardening law by which the experimental true stress and longitudinal true plastic strain are approximated; 2) parameters of the 3rd order polynomial fit by which the experimental transverse and longitudinal true plastic strains are approximated. Combined Swift-Voce hardening law reads

$$\sigma = c'(k(\bar{\varepsilon}_0^p + \varepsilon^p)^n) + (1-c')(R + Q(1-e^{-b\varepsilon^p})) \quad (9)$$

where $\bar{\varepsilon}_0^p$, R, Q, n, b and k are material parameters and c' is a weight factor. For the considered material these hardening parameters are given in Table 1 for seven tested specimen orientations.

For calculating r-values, incompressibility hypothesis is utilized and Eq. (6) is rewritten in the following form

$$r_\theta = -\frac{d\varepsilon_{\theta+90}^p}{d\varepsilon_{\theta+90}^p + d\varepsilon_\theta^p} = -\frac{m_\theta}{m_\theta + 1} \quad (10)$$

where $d\varepsilon_\theta^p$ and $d\varepsilon_{\theta+90}^p$ are the increments of true longitudinal and transverse plastic strains corresponding to the loading direction θ and direction $\theta+90^\circ$, respectively. According to Eq. (10), instantaneous r-values corresponding to the certain longitudinal true plastic strain can be calculated using the slope m_θ of the appropriate fit by which the experimental transverse and longitudinal true plastic strains are approximated. In the present paper, the 3rd order polynomial fit is utilized

$$Poly3(\varepsilon_\theta^p) = a + b\cdot\varepsilon_\theta^p + c\cdot(\varepsilon_\theta^p)^2 + d\cdot(\varepsilon_\theta^p)^3 \quad (11)$$

Parameters of the above polynomial function for all seven orientations are provided in Table 2.

Table 2. Parameters of Poly3 function for DC06 steel sheet [3]

$\theta(^\circ)$	a	b	c	d
0	0.0008	-0.6763	0.1343	0.0174
15	0.0005	-0.6619	0.0597	0.0941
30	0.0008	-0.6606	0.0153	0.1404
45	0.0003	-0.6806	0.0249	0.1241
60	0.0003	-0.7102	0.0425	0.1070
75	0.0005	-0.7309	0.0292	0.1243
90	0.0005	-0.7277	0.0088	0.1459

Following procedure presented in [3] based on the principle of the plastic work equivalence, from the above presented material data, instantaneous r-value and yield stress σ_y corresponding to the certain amount of the equivalent true plastic strain can be calculated. In the adopted approach, longitudinal true plastic strain in the rolling direction is used as the equivalent true plastic strain.

3.2 Evolution of Hill and Karafillis-Boyce yield function / plastic potential

In this paper, correlations of the Hill (1948) and Karafillis-Boyce (1993) yield function / plastic potential anisotropy parameters with the equivalent

plastic strain are derived. According to the adopted calculation procedure, yield stresses and *r*-values corresponding to the seven orientations (0°, 15°, 30°, 45°, 60°, 75° and 90°) and amounts of the equivalent plastic strain starting from 0.001 to 0.301 at each 0.002 increment are calculated. The calculated yield stress ratios (yield stresses normalized with yield stress for the rolling direction) and *r*-values corresponding to the selected equivalent plastic strain values are presented in Fig. 1 and Fig. 2, respectively.

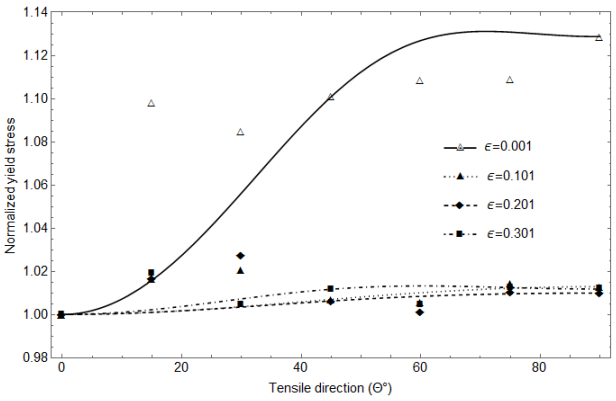

Figure 1. Yield stress ratio directional dependences corresponding to several values of equivalent plastic strain. Predictions of yield stress ratios by Hill yield function.

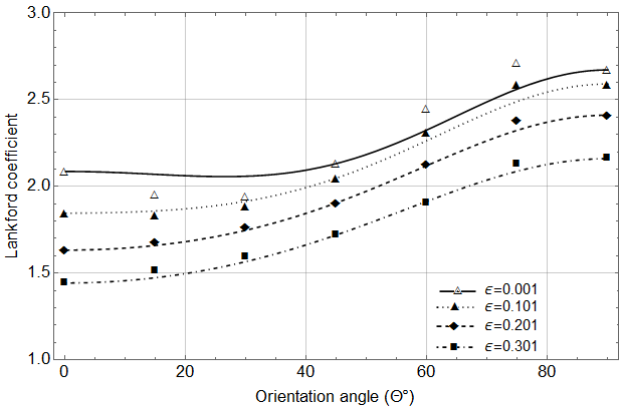

Figure 2. Lankford parameter directional dependences corresponding to several values of equivalent plastic strain. Predictions of Lankford parameters obtained by Hill plastic potential.

From Fig. 1 it can be observed that the directional dependence trend of the yield stress ratios at the start of plastic deformation ($\bar{\varepsilon}^p = 0.001$) is rather distorted with on-going plastic deformation process. Furthermore, a significant decrease of the *r*-values and evolution of *r*-value directional dependence with on-going deformation process can be observed in Fig. 2. In Figures 1 and 2 predictions of the yield stress and *r*-value directional dependences corresponding to the selected equivalent plastic strains obtained by the Hill yield function/plastic potential are also presented. The predictions of the Karafillis-Boyce yield function/plastic potential are almost identical to the predictions obtained by the Hill functions and therefore they are not separately presented. The anisotropy parameters of Hill and Karafillis-Boyce yield functions are calculated using the yield stresses corresponding to the orientations 0°, 45° and 90° ($\sigma_0, \sigma_{45}, \sigma_{90}$) and assuming that the yield stress at balanced biaxial stress state is the averaged value of the yield stresses corresponding to the longitudinal and transverse direction $\sigma_b = (\sigma_0 + \sigma_{90})/2$. The parameters of the Hill and Karafillis-Boyce plastic potentials are calculated using *r*-values corresponding to the orientations 0°, 45° and 90° (r_0, r_{45}, r_{90}). The function parameters are calculated for the equivalent plastic strains starting from 0.001 to 0.301 at each 0.002 increment.

The parameters corresponding to the selected plastic strain values for the analyzed yield functions/plastic potentials are presented in Table 3. From Fig. 1 it can be concluded that analyzed yield functions poorly predict the pronounced directional dependence at the onset of the plastic deformation process. For greater deformation levels, directional dependence is less pronounced and functions result in acceptable predictions. Figure 2 indicates that analyzed plastic potentials result in good predictions of the *r*-value directional dependence particularly for greater strain levels.

In order to relate the anisotropy parameters with the equivalent plastic strain, the fourth order polynomial fit is utilized. The utilized polynomial function is defined as

$$Poly4(\bar{\varepsilon}^p) = a + b_1 \cdot \bar{\varepsilon}^p + b_2 \cdot (\bar{\varepsilon}^p)^2 + b_3 \cdot (\bar{\varepsilon}^p)^3 + b_4 \cdot (\bar{\varepsilon}^p)^4 \quad (12)$$

The calculated polynomial parameters for the analyzed yield functions/plastic potentials are obtained using the least square method and are

presented in Table 4. Figures 3 and 4 show values of each anisotropy parameter corresponding to the several values of equivalent plastic strain and related polynomial fit. From these figures it can be observed that there is a good correlation between adopted fit and plastic potential parameters, while there is a certain discrepancy for yield function parameters for the lower plastic levels.

Table 3. Anisotropy parameters of Hill and Karafillis-Boyce yield function/plastic potential corresponding to several values of equivalent plastic strain

$\bar{\varepsilon}^p$	Hill yield function				Hill plastic potential function			
	λ_1	λ_2	ν	ρ	λ_1	λ_2	ν	ρ
0.001	1	0.784977	0.451113	1.208914	1	0.929017	0.676031	1.51877
0.101	1	0.974766	0.493752	1.478728	1	0.898972	0.648639	1.53337
0.201	1	0.980487	0.495158	1.480172	1	0.877411	0.620202	1.53260
0.301	1	0.976857	0.494265	1.459956	1	0.864181	0.590722	1.51627
$\bar{\varepsilon}^p$	Karafillis-Boyce yield function				Karafillis-Boyce plastic potential function			
	C	α_1	α_2	γ_3	C	α_1	α_2	γ_3
0.001	0.66602	0.884955	0.934993	1.3491	0.663130	0.9729273	0.8549610	1.51116
0.101	0.66665	0.987301	0.99356	1.48937	0.664162	0.9619441	0.8629602	1.51135
0.201	0.66666	0.990195	0.995045	1.49008	0.665051	0.9547230	0.8754240	1.50818
0.301	0.66665	0.98836	0.994106	1.47986	0.665764	0.9511359	0.8919975	1.50176

Table 4. Parameters of Poly4 fit for Hill and Karafillis-Boyce yield function/plastic potential

	Hill yield function				Hill plastic potential function			
	λ_1	λ_2	ν	ρ	λ_1	λ_2	ν	ρ
a	1	0.92024	0.481464	1.429272	1	0.9293305	0.67630	1.518681
b_1	0	3.52471	0.827483	4.650582	0	-0.345311	-0.26861	0.211961
b_2	0	-47.34067	-11.21203	-66.5226	0	0.4557313	-0.05202	-0.5717
b_3	0	225.4881	53.614063	323.6818	0	-0.157244	-0.00091	-1.00629
b_4	0	-351.6768	-83.800708	-512.050	0	0.2192994	0.00151	1.586853
	Karafillis-Boyce yield function				Karafillis-Boyce plastic potential function			
	C	α_1	α_2	γ_3	C	α_1	α_2	γ_3
a	0.6664	0.95801	0.9768	1.4632	0.6631	0.973044	0.854890	1.511186
b_1	0.0074	1.84314	1.0031	2.3715	0.0108	-0.129465	0.055896	0.016846
b_2	-0.0871	-24.6067	-13.2496	-33.751	-0.004	0.196509	0.245121	-0.13490
b_3	0.3861	116.8851	62.629	163.903	-0.009	-0.032977	-0.08198	-0.17842
b_4	-0.5770	-182.018	-97.2598	-259.026	0.0066	0.019654	0.038359	0.315813

Figures 5 and 6 present contours of the analyzed yield functions/plastic potentials in the normalized stress space for zero shear stress and corresponding to the selected equivalent plastic strains. For isotropic material, yield contours corresponding to the different amounts of plastic strain should coincide if presented in normalized stress space. From Fig. 5 discrepancy between initial yield contour and contours corresponding to the larger strain levels can be observed. Considering the analyzed plastic potentials, as shown in Fig. 6, there

is evolution of contour shape with ongoing deformation process.

This evolution is more pronounced for Hill plastic potential. These results are in correlation with the predictions presented in Figs. 1 and 2 and clearly indicate the use of the evolutionary anisotropic constitutive model.

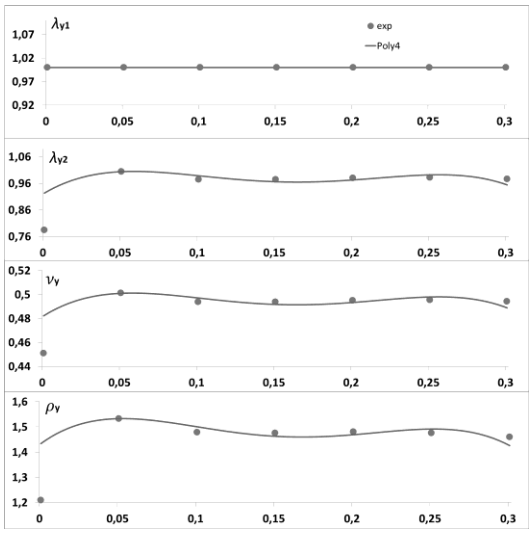

a)

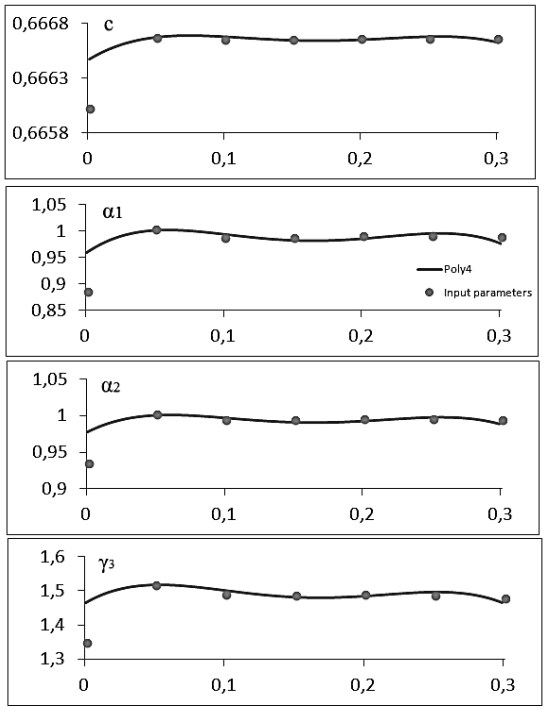

b)

Figure 3. Poly4 function fit for the anisotropy parameters of a) Hill and b) Karafillis Boyce yield function.

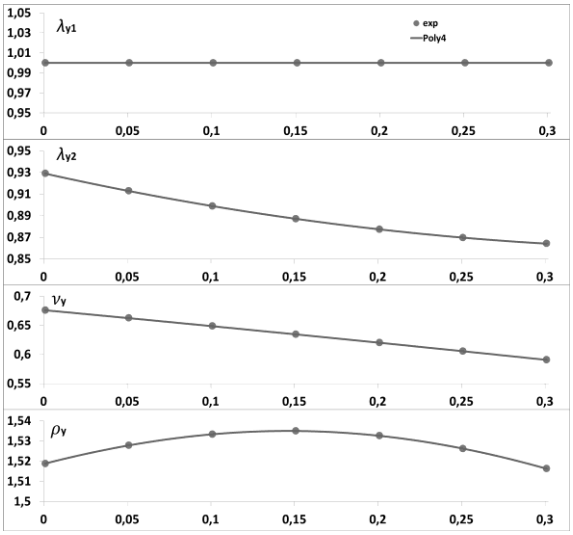

a)

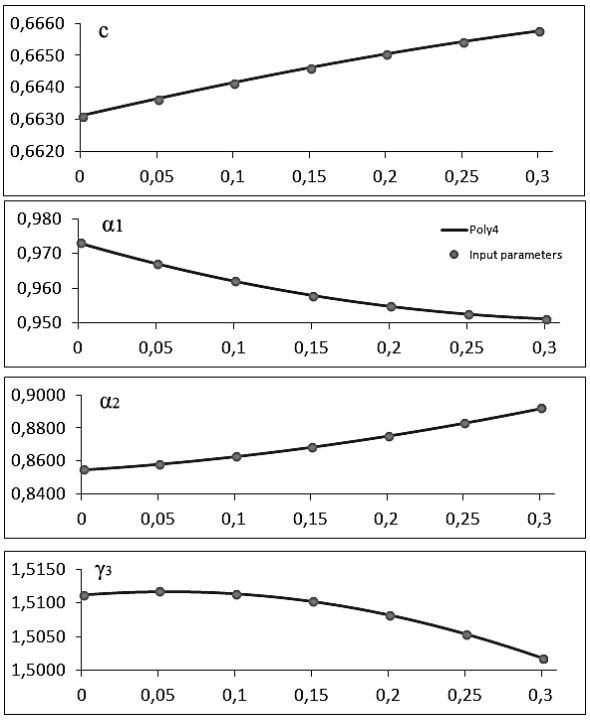

b)

Figure 4. Poly4 function fit for the anisotropy parameters of a) Hill b) Karafillis-Boyce plastic potential.

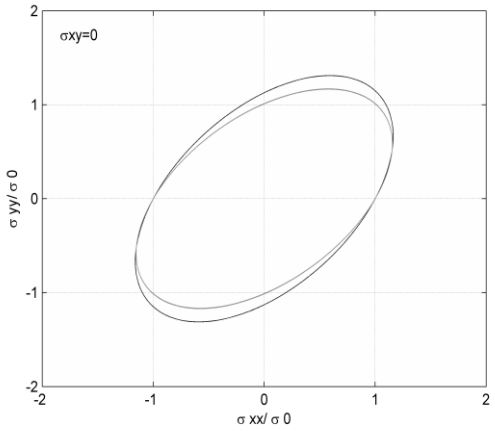

a)

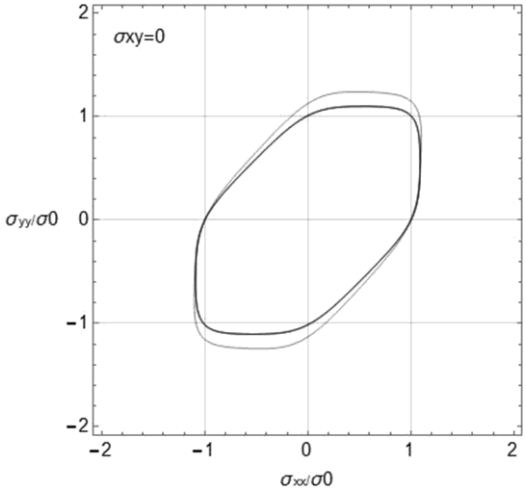

b)

Figure 5. Contours of a) Hill and b) Karafillis-Boyce yield function corresponding to $\bar{\varepsilon}^p = 0.001;\ 0.101;\ 0.201;\ 0.301$.

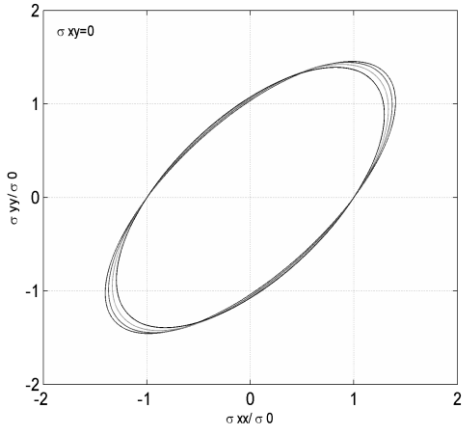

a)

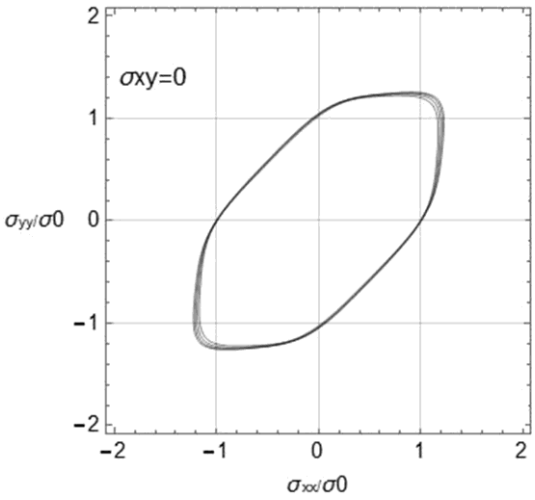

b)

Figure 6. Contours of a) Hill and b) Karafillis-Boyce plastic potential corresponding to $\bar{\varepsilon}^p = 0.001;\ 0.101;\ 0.201;\ 0.301$.

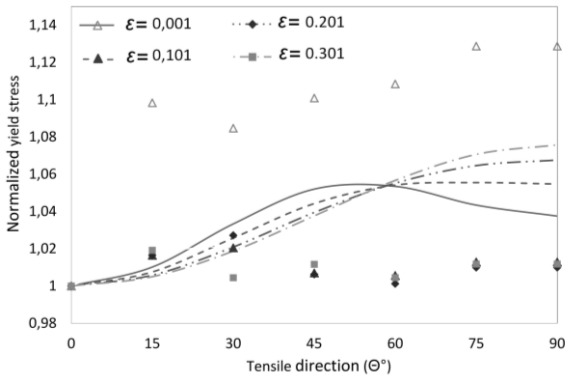

a)

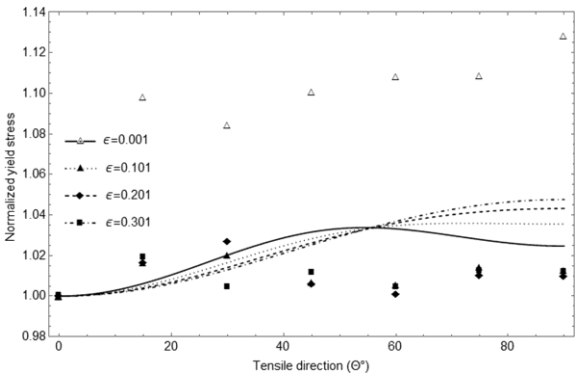

b)

Figure 7. Yield stress ratio directional dependences predicted by associated model and a) Hill and b) Karafillis-Boyce function adjusted to r-values corresponding to several values of the equivalent plastic strain.

Figure 7 presents predictions of the directional yield stress ratios obtained by the models based on the associated flow rule and Hill or Karafillis-Boyce stress function adjusted to *r*-values. Under the associated flow rule, stress function is utilized as yield function and as plastic potential function. It can be observed that such models poorly predict directional dependence of initial yield stresses as well as the alternation of the yield stress ratios with plastic deformation process.

4 Algorithmic formulation of the evolutionary anisotropic elasto-plastic constitutive model

4.1 Basic equations

Assuming isotropic linear elasticity and aditive decomposition of the strain tensor increment $d\boldsymbol{\varepsilon}$ into elastic $d\boldsymbol{\varepsilon}^{\mathbf{e}}$ and plastic part $d\boldsymbol{\varepsilon}^{\mathbf{p}}$, the stress tensor increment $d\boldsymbol{\sigma}$ reads

$$d\boldsymbol{\sigma} = \mathbf{C}^{\mathbf{e}} : d\boldsymbol{\varepsilon}^{\mathbf{e}} = \mathbf{C}^{\mathbf{e}} : (d\boldsymbol{\varepsilon} - d\boldsymbol{\varepsilon}^{\mathbf{p}}) \tag{13}$$

where $\mathbf{C}^{\mathbf{e}}$ is the tensor of elastic module. Considering sheet material with anisotropy evolution, the yield criterion is stated as follows

$$F = f_y(\boldsymbol{\sigma}, \bar{\varepsilon}^p) - \kappa(\bar{\varepsilon}^p) = 0 \tag{14}$$

where $f_y(\boldsymbol{\sigma}, \bar{\varepsilon}^p)$ is an orthotropic yield function with orthotropy parameters introduced as functions of hardening parameter $\bar{\varepsilon}^p$ and $\kappa(\bar{\varepsilon}^p)$ is a scalar function representing stress-strain relation for the referent direction. According to the plastic potential theory, the plastic part of the strain tensor increment $d\boldsymbol{\varepsilon}^{\mathbf{p}}$ is proportional to the gradient of the stress function named plastic potential function

$$d\boldsymbol{\varepsilon}^{\mathbf{p}} = d\lambda \frac{\partial f_p(\boldsymbol{\sigma}, \bar{\varepsilon}^p)}{\partial \boldsymbol{\sigma}} \tag{15}$$

where $d\lambda$ is a non-negative scalar called plastic multiplier or consistency parameter. Considering anisotropy evolution, plastic potential $f_p(\boldsymbol{\sigma}, \bar{\varepsilon}^p)$ is also introduced as an orthotropic stress function with orthotropy parameters stated as functions of the hardening variable $\bar{\varepsilon}^p$. If the plastic potential and yield function are identical $f_p(\boldsymbol{\sigma}, \bar{\varepsilon}^p) \equiv f_y(\boldsymbol{\sigma}, \bar{\varepsilon}^p)$, yielding and plastic flow are described by the same function and Eq. (15) becames the so-called associated flow rule. In the present formulation, the hardening parameter $\bar{\varepsilon}^p$ is considered as an equivalent plastic strain that obeys the principle of plastic work equivalence

$$f_y(\boldsymbol{\sigma}, \bar{\varepsilon}^p) d\bar{\varepsilon}^p = \boldsymbol{\sigma} : d\boldsymbol{\varepsilon}^{\mathbf{p}} \tag{16}$$

If the plastic potential function fulfils Euler's identity, the following evolution equation for the hardening parameter is obtained by using Eqs. (15) and (16)

$$\begin{aligned} f_y(\boldsymbol{\sigma}, \bar{\varepsilon}^p)\, d\bar{\varepsilon}^p &= d\lambda\ \boldsymbol{\sigma} : \frac{\partial f_p(\boldsymbol{\sigma}, \bar{\varepsilon}^p)}{\partial \boldsymbol{\sigma}} \\ &= d\lambda\ f_p(\boldsymbol{\sigma}, \bar{\varepsilon}^p) \end{aligned} \tag{17}$$

where for the associated flow rule $d\bar{\varepsilon}^p = d\lambda$. If deformation process is elastic, the incremental changes of the internal variables (plastic strain tensor and hardening parameter) vanish and $d\lambda = 0$. Therefore, for the hardening material the plastic multiplier obeys the complementary conditions $d\lambda \geq 0,\ F \leq 0,\ d\lambda F = 0$ and consistency condition $d\lambda\, dF = 0$.

4.2. Stress integration procedure

In the following, for the presented constitutive description that assumes distortion of the yield function/plastic potential, computational procedure for calculating state variables at time $t_{n+1}\,(\boldsymbol{\sigma}_{n+1}, \bar{\varepsilon}^p_{n+1})$ based on the known state variables at time $t_n\,(\boldsymbol{\sigma}_n, \bar{\varepsilon}^p_n)$ and known increment of total deformation $\Delta\boldsymbol{\varepsilon}$ is derived. The procedure is based on implicit return mapping [12], [13] and presents the extension of the procedures previously developed for the formulations based on isotropic hardening [5], [14]. By the application of the implicit return mapping procedure, the stress solution is obtained in two steps. In the elastic predictor step, the strain increment is assumed to be elastic and trial elastic stress tensor $\boldsymbol{\sigma}^{trial}$ is

calculated based on the previously converged solution

$$\boldsymbol{\sigma}^{trial} = \boldsymbol{\sigma}_n + \mathbf{C}^{\mathbf{e}} : \Delta\boldsymbol{\varepsilon} \tag{18}$$

If the trial state violates the yield condition, the plastic correction step is performed assuming trial state as initial condition. In this step the final stress is stated as

$$\boldsymbol{\sigma}_{n+1} = \boldsymbol{\sigma}_n + \mathbf{C}^{\mathbf{e}} : (\Delta\boldsymbol{\varepsilon} - \Delta\boldsymbol{\varepsilon}^{\mathbf{p}}) = \boldsymbol{\sigma}^{trial} - \mathbf{C}^{\mathbf{e}} : \Delta\boldsymbol{\varepsilon}^{\mathbf{p}} \tag{19}$$

and evolution equations for the internal variables are integrated to restore the consistency condition. By application of implicit Euler backward integration procedure and assuming associated flow rule, increment of plastic strain tensor is approximated as follows

$$\Delta\boldsymbol{\varepsilon}^{\mathbf{p}} = \Delta\lambda \mathbf{m}_{n+1}, \qquad \mathbf{m}_{n+1} = \left.\frac{\partial f_y(\boldsymbol{\sigma}, \bar{\varepsilon}^p)}{\partial \boldsymbol{\sigma}}\right|_{n+1} \tag{20}$$

Consistently, the increment of the hardening parameter is approximated as

$$\Delta\bar{\varepsilon}^p = \Delta\lambda \tag{21}$$

where $\Delta\lambda$ is an incremental consistency parameter that obeys discrete form of the complementary conditions $\Delta\lambda \geq 0, F(\boldsymbol{\sigma}_{n+1}, \bar{\varepsilon}^p_{n+1}) \leq 0,\ \Delta\lambda F(\boldsymbol{\sigma}_{n+1}, \bar{\varepsilon}^p_{n+1}) = 0$.

By using Eqs. (18) – (21), incremental form of the constitutive model can be stated by following system of non-linear equations

$$\Phi_1 \equiv f_y(\boldsymbol{\sigma}_{n+1}, \bar{\varepsilon}^p_n + \Delta\bar{\varepsilon}^p) - \rho_{n+1} = 0 \tag{22}$$

$$\boldsymbol{\Phi}_2 \equiv (\mathbf{C}^{\mathbf{e}})^{-1} : (\boldsymbol{\sigma}_{n+1} - \boldsymbol{\sigma}^{trial}) + \Delta\bar{\varepsilon}^p \mathbf{m}_{n+1} = 0 \tag{23}$$

$$\Phi_3 \equiv \rho_{n+1} - \kappa(\bar{\varepsilon}^p_n + \Delta\bar{\varepsilon}^p) = 0 \tag{24}$$

At each iteration k above three equations are linearized around the current values of state variables to obtain Eqs. (25) - (27). By solving obtained linearized system, explicit expressions Eqs. (28) - (30) for the increments of state variables are obtained

$$\Phi_1^{(k)} + \mathbf{m}^{(k)} : \Delta\boldsymbol{\sigma}^{(k)} + (\partial f_y / \partial \bar{\varepsilon}^p)^{(k)} \delta\Delta\bar{\varepsilon}^{p\,(k)} - \Delta\rho^{(k)} = 0 \tag{25}$$

$$\boldsymbol{\Phi}_2^{(k)} + (\mathbf{C}^{\mathbf{e}})^{-1} : \Delta\boldsymbol{\sigma}^{(k)} + \delta\Delta\bar{\varepsilon}^{p(k)} \mathbf{m}^{(k)} + \Delta\bar{\varepsilon}^{p(k)} (\partial\mathbf{m} / \partial\boldsymbol{\sigma})^{(k)} : \Delta\boldsymbol{\sigma}^{(k)} + \Delta\bar{\varepsilon}^{p(k)} (\partial\mathbf{m} / \partial\bar{\varepsilon}^p)^{(k)} \delta\Delta\bar{\varepsilon}^{p(k)} = 0 \tag{26}$$

$$\Phi_3 + \Delta\rho^{(k)} - (d\kappa / d\bar{\varepsilon}^p)^{(k)} \delta\Delta\bar{\varepsilon}^{p\,(k)} = 0 \tag{27}$$

$$\Delta\boldsymbol{\sigma}^{(k)} = -(\bar{\mathbf{C}}^{(k)})^{-1} : (\boldsymbol{\Phi}_2^{(k)} + (\mathbf{m}^{(k)} + \Delta\bar{\varepsilon}^{p(k)} (\partial\mathbf{m} / \partial\bar{\varepsilon}^p)^{(k)}) \delta\Delta\bar{\varepsilon}^{p(k)}) \tag{28}$$

$$\Delta\rho^{(k)} = -\Phi_3^{(k)} + (d\kappa / d\bar{\varepsilon}^p)^{(k)} \delta\Delta\bar{\varepsilon}^{p(k)} \tag{29}$$

$$\delta\Delta\varepsilon^{p(k)} = \frac{\Phi_1^{(k)} - \mathbf{m}^{(k)} : (\bar{\mathbf{C}}^{(k)})^{-1} : \boldsymbol{\Phi}_2^{(k)} + \Phi_3^{(k)}}{((d\kappa / d\bar{\varepsilon}^p)^{(k)} - (df_y / d\bar{\varepsilon}^p)^{(k)}) + \mathbf{m}^{(k)} : (\bar{\mathbf{C}}^{(k)})^{-1} : (\mathbf{m}^{(k)} + \Delta\bar{\varepsilon}^{p(k)} (\partial\mathbf{m} / \partial\bar{\varepsilon}^p)^{(k)})} \tag{30}$$

where $\bar{\mathbf{C}}^{(k)} = (\mathbf{C}^{\mathbf{e}})^{-1} + \Delta\bar{\varepsilon}^{p(k)} (\partial\mathbf{m} / \partial\boldsymbol{\sigma})^{(k)}$.

Finally, updated state variables are defined as

$$\begin{Bmatrix} \Delta\bar{\varepsilon}^p \\ \rho \\ \boldsymbol{\sigma} \end{Bmatrix}_{n+1}^{(k+1)} = \begin{Bmatrix} \Delta\bar{\varepsilon}^p \\ \rho \\ \boldsymbol{\sigma} \end{Bmatrix}_{n+1}^{(k)} + \begin{Bmatrix} \delta\Delta\bar{\varepsilon}^p \\ \Delta\rho \\ \Delta\boldsymbol{\sigma} \end{Bmatrix}_{n+1}^{(k)} \tag{31}$$

4.3 Numerical analysis of accuracy

In order to estimate the accuracy of the proposed algorithm based on distortional hardening model and associated flow rule, iso-error maps [12] are calculated. In the tested formulation, data for DC06 steel sheet presented in Section 3 are utilized: stress-strain relation for the rolling direction and polynomial relations for the anisotropic parameters of the Hill / Karafillis-Boyce function. Besides these data, following values are utilized for Young's modulus and Poisson's coefficient: $E = 200\,\text{GPa}$; ν=0.3. Iso-error maps are calculated at three representative stress points on the yield surface: A-uniaxial, B-balanced biaxial and C- pure shear as shown in Fig. 8. The strain increments ranging from zero to six times of the yield strain ε_y are applied to the considered stress points. The calculations are performed assuming $\Delta\varepsilon_{xy} = 0$ thus $\sigma_{xy} = 0$ applies. Iso-error maps are drawn based on the percentage of the relative mean square of errors between the computed stress $\boldsymbol{\sigma}$ and exact stress $\boldsymbol{\sigma}^*$

$$\delta(\%) = \frac{\sqrt{(\boldsymbol{\sigma}-\boldsymbol{\sigma}^*):(\boldsymbol{\sigma}-\boldsymbol{\sigma}^*)}}{\sqrt{\boldsymbol{\sigma}^*:\boldsymbol{\sigma}^*}} \cdot 100 \tag{32}$$

As the exact solution, the stresses obtained by 100 sub-steps for Hill formulation and 50 sub-steps for Karafillis-Boyce formulation of each strain increment are used. Figures 9 and 10 show the calculated iso-error maps obtained by the analyzed formulations. It can be observed that for points B and C, the axis of the exact solution are shifted to the stress symmetry axes. For both analyzed formulations, considering different stress points, it can be stated that the errors are relatively smaller for the biaxial stress state. Furthermore, it can be observed that for the formulation based on non-quadratic Karafillis-Boyce function a reduction in the strain increment does't intail a reduction in the error magnitude.

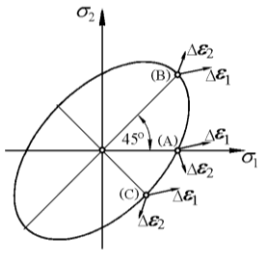

Figure 8. Plane stress yield surface and points A, B and C for iso-error maps.

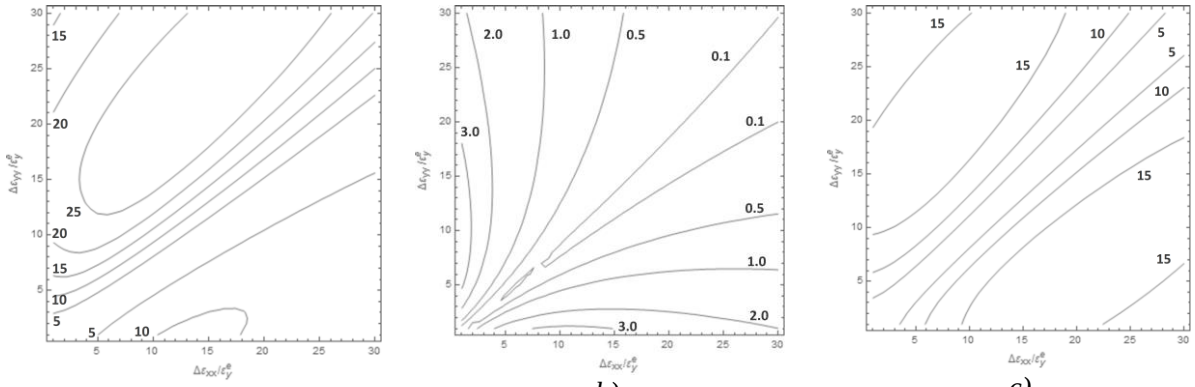

a) *b)* *c)*

Figure 9. Iso-error maps obtained by the Hill associated formulation based on the distortional hardening for points: (a) A; (b) B; (c) C.

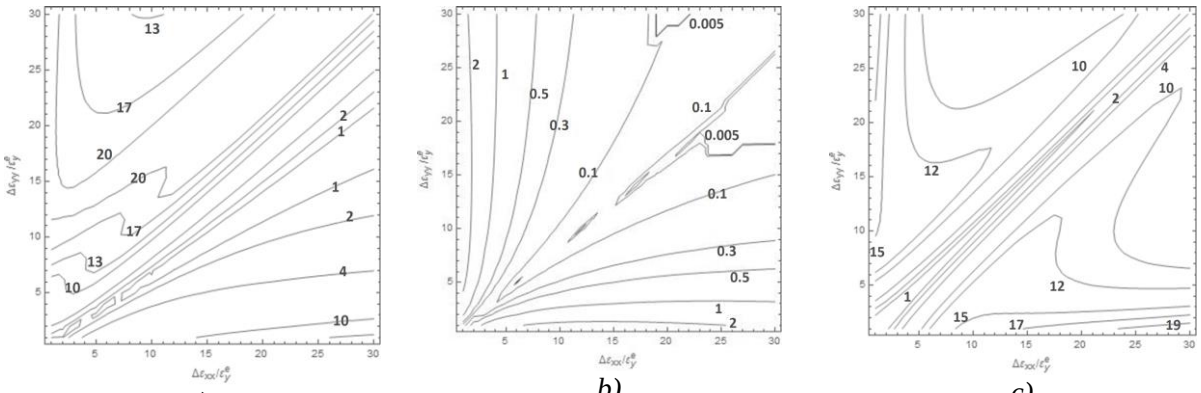

a) *b)* *c)*

Figure 10. Iso-error maps obtained by the Karafillis-Boyce associated formulation based on the distortional hardening for points: (a) A; (b) B; (c) C.

5 Conclusions

In the present paper, constitutive formulations based on the orthotropic Hill (1948) or Karafillis- Boyce (1993) stress functions that enable distortion of the yield function/plastic potential are presented and analyzed. The formulations based on the non-associated flow rule results in acceptable predictions of the yield stress and *r*-value directional dependences and their evolution with ongoing deformation for DC06 sheet steel sample. For the formulations based on associated flow rule, stress integration procedures are developed based on the implicit return mapping procedure. Accuracy of the derived computational procedures is estimated by calculating iso-error maps.

References

[1] An, Y. G., Vegter, H., Melzer, S., Triguero, P. R.: *Evolution of the plastic anisotropy with straining and its implication on formability for sheet metals*, Journal of Materials Processing Technology, 213 (2013), 8, 1419-1425.

[2] Zamiri, A., Pourboghrat, F.: *Characterization and development of an evolutionary yield function for the superconducting niobium sheet*, International Journal of Solids and Structures, 44 (2007), 26-27, 8627-8647.

[3] Safaei, M., Lee, M.-G., Zang S.-I., De Waele, W.: *An evolutionary anisotropic model for sheet metals based on non-associated flow rule approach*, Computational Materials Science, 81 (2014), 15-29.

[4] Yoon, J. W., Barlat, F., Dick, R. E., Karabin, M. E.: *Prediction of six or eight ears in a drawn cup based on a new anisotropic yield function*, International Journal of Plasticity, 22 (2016), 9, 174-193.

[5] Cvitanić, V., Vlak, F., Lozina, Ž.: *A finite element formulation based on non-associated plasticity for sheet metal forming*, International Journal of Plasticity, 24 (2008), 4, 646-687.

[6] Yoon, J. H., Cazacu, O., Yoon, J. W., Dick, R. E.: *Earing predicitons for strongly textured aluminium sheets*, International Journal of Mechanical Sciences, 52 (2010), 1563-1578.

[7] Aretz, H.: *A simple isotropic-distrotional hardening model and its application in elasto-plastic analysis of localized necking in orthotropic sheet metal*, International Journal of Plasticity, 24 (2008), 1457-1480.

[8] Plunkett, B., Cazacu, O., Lebensohn, R. A., Barlat, F.: *Evolving yield function of hexagonal materials taking into account texture development and anisotropic hardening*, Acta Mater., 54 (2006), 4159-4169.

[9] Hill, R.: *Theory of yielding and plastic flow of anisotropic metals*, Proc. Roy. Soc., 193 (1948), 281-297.

[10] Karafillis, A. P., Boyce, M.: *A general anisotropic yield criterion using bounds and a transformation weighting tensor*, J. Mech. Phys. Solids, 41 (1993), 1859-1886.

[11] Barlat, F., Brem, J. C., Yoon, J. W., Chung, K., Dick, R. E., Lege, D. J., Pourboghrat, F., Choi, S. H., Chu, E.: *Plane stress yield function for aluminum alloy sheets - part 1: theory*, International Journal of Plasticity, 19 (2003), 9, 1297-1319.

[12] Simo, J.C., Hughes T.J.R.: *Elastoplasticity and viscoplasticity - Computational aspects*, Springer-Verlag, 1988.

[13] Yoon, J. W., Yang, D. Y., Chung, K.: *Elasto-plastic finite element method based on incremental deformation theory and continuum based shell elements for planar anisotropic sheet materials*, Comp. Methods in Applied Mechanics and Engineering, 174 (1999), 23-56.

[14] Cvitanić, V., Lozina, Ž., Vlak, F.: *Application of non-associated flow rule to sheet metal forming*, Proceedings of the 5th International Congress of Croatia Society of Mechanics, Croatian Society of Mechanic, Trogir, Croatia, 2006, 147-148.